



TECHNISCHE UNIVERSITÄT CHEMNITZ

Sonderforschungsbereich 393

Parallele Numerische Simulation für Physik und Kontinuumsmechanik

Peter Benner

Jens Saak

Linear-Quadratic Regulator Design for Optimal Cooling of Steel Profiles

Preprint SFB393/05-05

Abstract

We present a linear-quadratic regulator (LQR) design for a heat transfer model describing the cooling process of steel profiles in a rolling mill. Primarily we consider a feedback control approach for a linearization of the nonlinear model given there, but we will also present first ideas how to use local (in time) linearizations to treat the nonlinear equation with a regulator approach. Numerical results based on a spatial finite element discretization and a numerical algorithm for solving large-scale algebraic Riccati equations are presented both for the linear and nonlinear models.

Key words. Dynamical linear systems, 2-D heat equation, feedback control, boundary control, Riccati operators, approximation schemes

AMS subject classification. 49J20, 65K10, 93B40

Preprintreihe des Chemnitzer SFB 393

ISSN 1619-7178 (Print)

ISSN 1619-7186 (Internet)

SFB393/05-05

April 2005

Contents

1	Introduction	1
1.1	Notations and Basic Properties	1
2	Mathematical Model	2
2.1	Model Background	2
2.2	Model Equation	3
2.3	Boundary Conditions and Boundary Control	4
2.4	Choice of State Weights Q and Output C	5
2.5	Units of Measurement and Scaling	6
3	Theoretical Background	7
3.1	Linear-Quadratic Regulator Problems in Hilbert Spaces	7
3.2	Weak Formulation and Abstract Cauchy Problem	8
3.3	Approximation by Finite Dimensional Systems	10
4	Theoretical Results	11
5	Implementation details	12
6	Numerical results	14
7	Conclusions	17

Author's addresses:

Peter Benner and Jens Saak:
Fakultät für Mathematik,
Technische Universität Chemnitz,
D-09107 Chemnitz, Germany;
{benner, jens.saak}@mathematik.tu-chemnitz.de.

1 Introduction

We present a method to treat linear and nonlinear boundary control problems for the heat equation, arising in the selective cooling of steel profiles, with a regulator approach. The particular objectives of this publication will be to present the theoretical background in case of a linear problem and show first ideas considering the treatment of the nonlinear version. We also review the numerical methods used to solve the high dimensional regulator problem.

The basic model has been described in detail in [21, 8, 11] and references therein. Various control strategies and techniques have been discussed including continuous (e.g. [21]) and discontinuous (e.g. [8]) intensity regulation for the cooling nozzles that spray the cooling fluid onto the surface of the profile. In contrast to the methods used in [21, 8, 11] we want to establish the control by a feedback law. For designing the control law we restrict ourselves to the linear case. Taking a quadratic cost functional and making a spatial semi-discretization of the model equation we end up with a linear quadratic regulator (LQR) problem for a system of ordinary differential equations of large dimension. This can at least theoretically be treated with standard methods. From the computational point of view the complexity of classical methods for solving the LQR problem makes it infeasible to implement this approach. Therefore, we choose the method proposed in [4], which exploits the sparsity and structure of the matrices involved, to solve the corresponding algebraic Riccati equation.

The presented approach is not limited to the application to linear heat transfer processes, but can in principle be used to solve a variety of linear-quadratic optimal control problems for parabolic processes. We chose the optimal steel cooling problem as it allows to demonstrate that the LQR approach—in contrast to common belief—is applicable to concrete control applications described by partial differential equations. In particular, we can compare our results at least on a qualitative level to other control and optimization strategies for the same problem as such results are available in the open literature, see [8, 9, 21].

1.1 Notations and Basic Properties

Throughout this paper we will denote by $\mathbb{R}^{m,n}$ the space of $m \times n$ real matrices. The complex plane is denoted by \mathbb{C} and the open left half-plane by \mathbb{C}^- . For a matrix $A \in \mathbb{R}^{m,n}$, A^T stands for the transpose. The identity matrix of order n is denoted by I_n or just I if dimensions are evident. In case of an operator A the Hilbert space adjoint is denoted by A^* . In both cases we write $\text{rg}(A)$ for the range, $\ker(A)$ for the null space, and $\text{dom}(A)$ for the domain of A .

By $H^{m,p}(\Omega)$ we denote the Sobolev space $H^{m,p}(\Omega) = \{u \in L^p(\Omega) : |\alpha| \leq m, \partial^\alpha u \in L^p(\Omega)\}$ of m -times weakly differentiable functions in $L^p(\Omega)$ with its norm $\|u\|_{m,p} := \left(\sum_{|\alpha| \leq m} \int_{\Omega} |\partial^\alpha u(x)|^p dx \right)^{\frac{1}{p}}$.

In general we will restrict ourself to the case of Hilbert spaces where $p = 2$ and the scalar product is $(u, v)_{m,2} := \left(\sum_{|\alpha| \leq m} \int_{\Omega} \partial^\alpha u(x) \partial^\alpha v(x) dx \right)^{\frac{1}{2}}$. We then write $H^m(\Omega) := H^{m,2}(\Omega)$. These

spaces are appropriate to describe solutions of the elliptic equation associated to the parabolic problem. Let $[t_0, T) \subset \mathbb{R}$ be the time interval of interest. We will then write $H^1([t_0, T); H^1(\Omega))$ for the H^1 -space defined with respect to the Bochner-integral analogously to the one above which uses Lebesgue-integrals, see, e.g., [22].

We denote the space of *linear, bounded operators* from a Banach space X to a Banach space Y by $\mathcal{L}(X, Y)$ and its subspace of compact operators by $\mathcal{K}(X, Y)$. In case $Y = X$ we simply write $\mathcal{L}(X)$ and $\mathcal{K}(X)$. Following the notation in [15] we call a linear operator A *dissipative* if for every $x \in \text{dom}(A) \subset X$ there exists $x^* \in X^*$ with $\langle x^*, x \rangle = \|x\|^2 = \|x^*\|^2$ and $\text{Re} \langle Ax, x^* \rangle \leq 0$, where the duality product $\langle \cdot, \cdot \rangle$ is defined via $\langle x^*, x \rangle := x^*(x)$.

We close this section with a helpful result [15, Corollary 4.4; Section 1.4] we will need later.

Proposition 1.1. *Let A be a densely defined closed linear operator on a Banach space X . If both A and A^* are dissipative, then A is the infinitesimal generator of a strongly continuous (\mathbb{C}^0-) semigroup of contractions on X .*

For additional information on semigroups of operators we refer the reader to [7, 15].

The remainder of this paper is structured as follows. The following section introduces the mathematical model and boundary conditions. It will also show how the nonlinear equation and boundary conditions have to be linearized to be able to formulate the linear quadratic feedback control system. Furthermore the design of the cost functional is discussed and scaling aspects are treated. Section 3 then shows the theoretical background and formulates the abstract Cauchy problem used to describe the infinite dimensional control problem. In Section 4 the main approximation result is given. Sections 5 and 6 present implementation details and results of the numerical tests. We close with some final remarks and conclusions in Section 7.

2 Mathematical Model

2.1 Model Background

We consider the problem of optimal cooling of steel profiles. This problem arises in a rolling mill when different steps in the production process require different temperatures of the raw material. To achieve a high production rate, economical interests suggest to reduce the temperature as fast as possible to the required level before entering the next production phase.

At the same time, the cooling process, which is realized by spraying cooling fluids onto the surface, has to be controlled so that material properties, such as durability or porosity, achieve given quality standards. Large gradients in the temperature distributions within the steel profile may lead to unwanted deformations, brittleness, loss of rigidity, and other undesirable

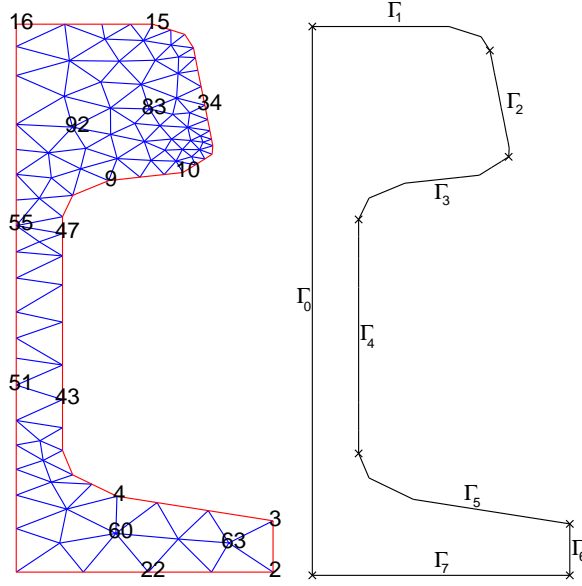


Figure 1: initial mesh with points of minimization and comparison (left) and partition of the boundary (right).

material properties. It is therefore the engineers goal to have a preferably even temperature distribution.

2.2 Model Equation

As in [8, 9, 11, 21] the steel profile is assumed to stretch infinitely into the z -direction which is justified by comparing the actual length of steel profiles like rails to their width and height. This admits the assumption of a stationary heat distribution in z -direction, or in other words, we can restrict ourselves to a 2-dimensional heat diffusion process. Therefore, we can consider the 2-dimensional cross-sections of the profile $\Omega \subset \mathbb{R}^2$ shown in Figure 1 as computational domain. Measurements for defining the geometry of the cross-section are taken from [21]. As one can see the domain exploits the symmetry of the profile introducing an artificial boundary Γ_0 on the symmetry axis. The state equation introduced in [21, 8, 11] for the temperature $x(\xi, t)$ at time t in point ξ can be summarized as follows:

$$\begin{aligned} c(x)\rho(x)x_t(\xi, t) &= \nabla \cdot (\lambda(x)\nabla x(\xi, t)) && \text{in } \Omega \times (0, T), \\ -\lambda(x)\partial_\nu x(\xi, t) &= g_i(\xi, t, x, u) && \text{on } \Gamma_i \times (0, T), \\ x(\xi, 0) &= x_0(\xi) && \text{in } \Omega, \end{aligned} \quad (1)$$

where g_i includes temperature differences between cooling fluid and profile surface, intensity parameters for the cooling nozzles and heat transfer coefficients modeling the heat transfer to the cooling fluid. We will present some variants of this boundary condition in Section 2.3.

We will mostly use the linearized version of the above state equation given in (2). The linearization is derived from (1) by taking means of the material parameters ρ , λ and c . This is admissible as long as we work in temperature regimes above 700°C where changes of ρ , λ and c are small and we do not have multiple phases and phase transitions in the material. Furthermore we partition the boundary into 8 parts, where one of these is the artificial boundary on the left hand side of Ω . The others are located between two neighboring corners of the domain and are enumerated clockwise (see Figure 1 for details). Another simplification taken here is the assumption that the cooling nozzles spray constantly onto one part of the surface. This means u is constant with respect to the spatial variable ξ on each part Γ_i of the boundary. Thus we obtain the following model:

$$\begin{aligned} c\rho x_t(\xi, t) &= \nabla \cdot (\lambda \nabla x(\xi, t)) && \text{in } \Omega \times (0, T) \\ -\lambda \partial_\nu x(\xi, t) &= g_i(t, x, u) && \text{on } \Gamma_i \text{ where } i = 0, \dots, 7 \\ x(\xi, 0) &= x_0(\xi) && \text{in } \Omega. \end{aligned} \quad (2)$$

Throughout this paper we will consider the following cost functional:

$$\mathcal{J}(x_0, u) := \int_0^\infty (x, Qx)_H + (u, Ru)_U dt. \quad (3)$$

in which Q and R can be chosen to weight temperature differences and the cost of spraying the cooling fluid. The control problem of interest can thus be summarized as

$$\begin{aligned} &\text{Minimize (3) with respect to (2), where } Q \text{ is given as } Q := C^*C \text{ or } Q := C^*\hat{Q}C \\ &\text{with } \hat{Q} \geq 0. \end{aligned} \quad (\mathcal{R})$$

We will specify C and \hat{Q} in more detail later.

2.3 Boundary Conditions and Boundary Control

We now have to describe the heat transfer across the surface of the material, i.e. the boundary conditions. The most general way to model the heat flux across the boundary is a combination of heat conduction and radiation. The heat conduction is modeled proportional to the difference between surface temperature and exterior temperature, where the proportionality coefficient is the heat transfer coefficient κ depending on the material of the profile, the type of cooling fluid that is used, the temperatures of profile and fluid and also on the spraying intensity. The radiation of heat is given by the Stefan-Boltzmann law. So we end up with

$$-\lambda \partial_\nu x(\xi) = g_i(t, u) := \kappa_k(x - x_{ext,k}) + \varepsilon \sigma (x^4 - x_{ext,k}^4), \quad k = 1, \dots, 7, \quad (4)$$

where $\sigma = 5.660 \cdot 10^{-8} \text{W/m}^2\text{K}^4$ is the Stefan-Boltzmann constant and $\varepsilon \in [0, 1]$ ($\varepsilon = 1$ for an ideal black body, so we should expect $\varepsilon < 1$ here.).

The boundary condition (4) is nonlinear and thus must be linearized if we want to use LQR design for linear systems. Therefore we will simplify it by dropping the Stefan-Boltzmann part.

This is not too much of an error because that term is much smaller than the conduction part, at least in case of active cooling.

$$-\lambda \partial_\nu x(\xi) = \kappa_k(x - x_{ext,k}) \quad (5)$$

We now have two choices for selecting the control variables. The most intuitive choice concerning the presented model problem is to regulate the intensity of the spraying nozzles. This idea results in taking the heat transfer coefficient κ as the control. As we will see later in detail this leads to a problem with the formulation of the linear feedback control system. Instead of a linear system we have to consider a bilinear system with this choice which results from the multiplication of the control and the state on the right hand side of (5).

Another possibility is to take the external temperature as the control. In our example this means we regulate the temperature of the cooling fluid which is sprayed onto the steel profile. This might lead to complications with the technical realization of the model because in this application it will possibly be difficult to achieve the reaction times calculated by the model. On the other hand we can think of applications of the present theory to the modeling and control of air conditioning systems. There, reaction times are much longer and this choice would most likely be the best one in that case. The mathematical advantage of this choice is that the multiplication of control and state which lead to the difficulties in the above case are bypassed here.

A third possibility would be to write (5) as $-\lambda \partial_\nu x(\xi) = \kappa_1 x - \kappa_2 x_{ext,k}$ and replace κ_1 by an appropriate constant, e.g., some kind of mean. We could then use κ_2 as the control, but this is equivalent to controlling by means of the exterior temperature in the formulation above. Having κ_1 fixed we can rewrite $\kappa_2 = \kappa_1 * \hat{\kappa}_2$ and define $\hat{u}_{ext,k} := \hat{\kappa}_2 u_{ext,k}$, i.e. we can use $\hat{u}_{ext,k}$ as the control like in (5).

2.4 Choice of State Weights Q and Output C

In (R) we already mentioned that the control weighting operator/matrix Q should be chosen as $Q := C^*C$ or $Q := C^*\hat{Q}C$. We will now show in more detail how we choose C and \hat{Q} . As it was mentioned in Section 2.1, an even temperature distribution on cross-sections of the profile at the end of the cooling process is desired. We want to take this fact into account by introducing certain temperature differences in the cost functional. We approximate gradients by simple differences because this turns out to be sufficient to accomplish the given task. Additionally, temperature difference calculations are cheaper to compute and easier to implement. So concerning implementation they are the primary choice here.

On the other hand this leads to slight complications in the theoretical part. We would like to evaluate the state function in single nodes of the coarsest grid, to know the temperature in a specific point. We use nodes of the coarsest grid here, because those are present on every refinement level created by our finite element method. Unfortunately the regularity of the solution is not sufficient to allow those evaluations. We do not have H^2 -regularity of the

solution, since the boundary is not smooth enough (because of the two sharp corners at the ends of Γ_6) and boundary conditions may jump in the interconnection points between two parts of the boundary. Therefore we do not have continuity and can not evaluate the state function in single points, but we can evaluate integrals of the state over small regions in Ω . This problem is solved by defining C according to differences between integral means on small ε -balls around the desired grid nodes. That means if we are interested in the temperature at the i -th grid node with coordinates $\xi_i \in \Omega$ we consider

$$\eta_i := \frac{1}{|B_\varepsilon(\xi_i)|} \int_{B_\varepsilon(\xi_i)} x(\xi) d\xi. \quad (6)$$

With this notation we define

$$C : H \rightarrow \mathbb{R}^6$$

$$x \mapsto C(x) := \begin{bmatrix} 3\eta_{60} - \eta_{22} - \eta_4 \\ 2\eta_{63} - \eta_3 - \eta_2 \\ \eta_{51} - \eta_{43} \\ 2\eta_{92} - \eta_9 - \eta_{16} \\ 3\eta_{83} - \eta_{34} - \eta_{10} - \eta_{15} \end{bmatrix} \quad (7)$$

The grid nodes referred to in the above definition can be found in Figure 1. The lines of $C(x)$ in (7) have to be read as: Take the Difference of the temperature integrals (6) for nodes 63 and 3 as well as the difference for nodes 63 and 2 (if we look at line 2 as an example) and add them. Note that we placed an additional weight on the temperature around node 60 in line 1 of $C(x)$. This turned out to be important to get the profile's foot appropriately cooled down with the given cost functional, see the plots in the results section of [5] for details. Concerning \hat{Q} we think of choosing $\hat{Q} := \beta I$ for some positive real constant β . β can then be used as a weighting factor to prioritize states over controls or the contrary in the cost functional. Alternative choices for \hat{Q} might be diagonal matrices where the diagonal entries are then weighting factors for the temperature differences in relation to each other. For example one might want to devalue the differences on the web against those in the head of the profile, because temperature differences normally tend to be much smaller on the web than in the head.

2.5 Units of Measurement and Scaling

The final paragraph of this model introduction section will now concern units of measurement. We have introduced the model without too much concern about measurements until here. For the implementation we want to rescale the temperature regime from the interval $[0, 1000]$ °C to the unit interval $[0, 1]$ and the lengths from meters to decimeters. We are especially interested in the effect this rescaling has on the time scale. To answer this question we first list the parameters again with their units of measurement:

- specific density ϱ in $\frac{kg}{m^3}$,

- specific heat capacity c in $\frac{m^2}{s^2}$,
- heat conductivity λ in $\frac{kg\ m}{s^3}$,
- heat transfer coefficient κ in $\frac{kg}{s^3}$.

For $\alpha = \frac{\lambda}{c\varrho}$ this leads to

$$\frac{\frac{kg\ m}{s^3\ ^\circ C}}{\frac{m^2}{s^2\ ^\circ C} \frac{kg}{m^3}} = \frac{m^2}{s},$$

So the rescaling of temperature has no effect on the other units, for it cancels out in the above computation. The rescaling of lengths on the other hand has to be taken into account even squared. If we do this we can take the original values of λ , c , ϱ and κ for the numerical tests. Dividing by $-\lambda$, (5) becomes $\partial_\nu x = \frac{\kappa}{\lambda}(x_{ext} - x)$. So we have to take a closer look at the coefficient $\frac{\kappa}{\lambda}$. This has the unit of measurement

$$\frac{\frac{kg}{s^3\ ^\circ C}}{\frac{kg\ m}{s^3\ ^\circ C}} = \frac{1}{m}.$$

Hence we do not have to take the rescaling into account, because the normal ν on the left and the coefficient $\frac{\kappa}{\lambda}$ scale with the same factor.

3 Theoretical Background

The theoretical fundament for our approach was set by Gibson [10]. The ideas and proofs used for the boundary control problem considered here closely follow the extension of Gibson's method proposed by Banks and Kunisch [1] for distributed control systems arising from parabolic equations. Similar approaches can be found in [12]. Common to all those approaches is to formulate the control system for a parabolic system as an abstract Cauchy problem in an appropriate Hilbert space setting. For numerical approaches this Hilbert space is approximated by a sequence of finite dimensional spaces, e.g. by spatial finite element approximations, leading to large sparse systems of ordinary differential equations in \mathbb{R}^n . Following the theory in [1] those approximations do not even have to be subspaces of the Hilbert space of solutions.

3.1 Linear-Quadratic Regulator Problems in Hilbert Spaces

In the remainder of this publication we will assume that the state space H , the input space U and the output space O are Hilbert spaces. For operators $A \in \mathcal{L}(\text{dom}(A), H)$ and $B \in \mathcal{L}(U, H)$ with $\text{dom}(A) \subset H$ and A the infinitesimal generator of the \mathcal{C}^0 -semigroup $T(t)$ on H , we examine

the system

$$\begin{aligned} \dot{x}(t) &= Ax(t) + Bu(t), & \text{for } t > 0, \\ y(t) &= Cx(t), & \text{for } t > 0, \\ x(0) &= x_0. \end{aligned} \tag{8}$$

Furthermore we consider the cost functional (3) for selfadjoint operators $Q \in \mathcal{L}(H)$ and $R \in \mathcal{L}(U)$, with $Q \geq 0$ and $R > 0$. This completes the LQR-problem:

$$\text{Minimize (3) over } u \in L^2(0, \infty; U) \text{ with respect to (8).} \tag{\mathfrak{R}^{\mathcal{J}^c}}$$

Let $A : H \rightarrow H$ be the infinitesimal generator of a \mathcal{C}^0 -semigroup $T(t)$, $B : U \rightarrow H$ the above input operator. From [10] we know that the solution trajectory x_* and control input u_* can be expressed by

$$\begin{aligned} u_*(t) &= -R^{-1}B^*\Pi_\infty x_*(t) \\ x_*(t) &= S(t)x_0 \end{aligned} \tag{9}$$

iff there exists an admissible control for (3),(8) for every $x_0 \in H$. Here Π_∞ is the minimum nonnegative selfadjoint solution of the operator algebraic Riccati equation:

$$\mathfrak{R}(\Pi) := Q + A^*\Pi + \Pi A - \Pi B R^{-1} B^* \Pi = 0 \tag{10}$$

in the sense that for all $\varphi, \psi \in \text{dom}(A)$ it holds

$$(\varphi, Q\psi)_H + (A\varphi, \Pi\psi)_H + (\Pi\varphi, A\psi)_H - (B^*\Pi\varphi, B^*\Pi\psi)_U = 0$$

and $S(t)$ is the \mathcal{C}^0 -semigroup generated by $A - BR^{-1}B^*\Pi_\infty$. If $Q > 0$ then S is even uniformly exponentially stable.

3.2 Weak Formulation and Abstract Cauchy Problem

We will now show the relation of the abstract Cauchy problem (8) to the partial differential equation model problem from equation (2). We therefore consider a variational formulation of (2) tested with $v \in H^1(\Omega)$. We will later choose Galerkin approximations of $H^1(\Omega)$ as test spaces and thus get a finite dimensional approximation of the resulting Cauchy problem by choosing those Galerkin approximations as certain finite-element (fem) spaces. The weak formulation of (2) leads to

$$\begin{aligned} (\partial_t x, v) &= \left(\frac{1}{c\rho} \nabla \cdot \lambda \nabla x, v \right) \\ &= \int_{\Omega} \frac{1}{c\rho} (\nabla \cdot \lambda \nabla x) v d\xi = - \int_{\Omega} \alpha \nabla x \cdot \nabla v d\xi + \int_{\Gamma} \alpha \partial_\nu x v d\sigma \\ \stackrel{(5)}{=} & - \int_{\Omega} \alpha \nabla x \cdot \nabla v d\xi - \sum_{k=1}^7 \int_{\Gamma_k} \frac{\kappa_k}{c\rho} (x - x_{ext,k}) v d\sigma \\ &= - \int_{\Omega} \alpha \nabla x \cdot \nabla v d\xi - \sum_{k=1}^7 \left(\int_{\Gamma_k} \frac{\kappa_k}{c\rho} x v d\sigma - \kappa_k x_{ext,k} \int_{\Gamma_k} \frac{1}{c\rho} v d\sigma \right). \end{aligned} \tag{11}$$

Rewriting (11) as

$$(\partial_t x, v)_{L^2(\Omega)} + \alpha(\nabla x, \nabla v)_{L^2(\Omega)} + \sum_{k=1}^7 \frac{\kappa_k}{c\rho} (\text{tr } x, \text{tr } v)_{L^2(\Gamma_k)} - \sum_{k=1}^7 \frac{\kappa_k}{c\rho} (x_{ext,k}, \text{tr } v)_{L^2(\Gamma_k)} = 0 \quad (12)$$

with $\text{tr} : H^1(\Omega) \rightarrow L^2(\partial\Omega)$ the trace operator, and defining

$$\begin{aligned} A : H^1(\Omega) &\rightarrow H^1(\Omega)' \\ x &\mapsto \alpha \left((\nabla x, \nabla \cdot)_{L^2(\Omega)} - \sum_{k=1}^7 \frac{\kappa_k}{\lambda} (\text{tr } x, \text{tr } \cdot)_{L^2(\Gamma_k)} \right) \\ B : U &\rightarrow H^1(\Omega)' \\ x_{ext} &\mapsto \sum_{k=1}^7 \frac{\kappa_k}{c\rho} (x_{ext,k}, \text{tr } \cdot)_{L^2(\Gamma_k)} \\ M : H^1(\Omega) &\rightarrow H^1(\Omega)' \\ x &\mapsto (\partial_t x, \cdot)_{L^2(\Omega)'} \end{aligned} \quad (13)$$

we obtain the sesquilinear form

$$\sigma_A(\varphi, \psi) := \langle A\varphi, \psi \rangle + \alpha(\varphi, \psi)_{L^2(\Omega)} \quad (14)$$

where $\langle \varphi, \psi \rangle := \varphi(\psi)$ is the duality product for $\varphi \in H^1(\Omega)'$ and $\psi \in H^1(\Omega)$.

σ_A is a continuous and coercive sesquilinear form on $H^1(\Omega)$ because by definition it holds

$$\sigma_A(\varphi, \varphi) = \alpha \left(\|\varphi\|_{1,2}^2 + \sum_{k=1}^7 \frac{\kappa_k}{\lambda} \|\text{tr } \varphi\|_{L^2(\Gamma_k)}^2 \right)$$

so that obviously $\sigma_A(\varphi, \varphi) \geq \alpha \|\varphi\|_{1,2}^2$. The continuity of σ_A follows from the continuity of the trace operator (see, e.g., [22]). Now the theorem of Lax-Milgram guarantees the existence of invertible linear and bounded operators $A_\alpha \in \mathcal{L}(H^1(\Omega))$ and $A_\alpha^* \in \mathcal{L}(H^1(\Omega))$ such that

$$\begin{aligned} \sigma_A(\varphi, \psi) &= (-A_\alpha \varphi, \psi)_{H^1(\Omega)}, \\ \overline{\sigma_A(\varphi, \psi)} &= (-A_\alpha^* \psi, \varphi)_{H^1(\Omega)}. \end{aligned} \quad (15)$$

This results in a system of the form (8) with $H = H^1(\Omega)$, for (12) together with the initial conditions of the PDE now are:

$$\begin{aligned} \dot{x} &= A_\alpha x + B x_{ext} && \text{in } \Omega, \\ x(0, \cdot) &= x_0 && \text{in } \Omega \end{aligned} \quad (16)$$

In the definitions in (13) we implicitly used $u_{ext,k}$ ($k = 1, \dots, 7$) as the controls. If we chose to use the heat transfer coefficients κ_k as controls, we have to define A and B as follows

$$\begin{aligned} A : H^1(\Omega) &\rightarrow H^1(\Omega)' \\ x &\mapsto \alpha(\nabla x, \nabla \cdot)_{L^2(\Omega)} \\ B : U &\rightarrow H^1(\Omega)' \\ \kappa_k &\mapsto \sum_{k=1}^7 \frac{\kappa_k}{c\rho} (\text{tr } x - x_{ext,k}, \text{tr } \cdot)_{L^2(\Gamma_k)}. \end{aligned} \quad (17)$$

Thus B is actually $B(x)$ and the state equation becomes

$$\dot{x} = A_\alpha x + B(x)\kappa_k \text{ in } \Omega, \quad (18)$$

so that in this case we end up with a bilinear system and can not directly apply the linear theory. Eppler and Tröltzsch [9] avoid the bilinear control system by replacing the right hand side of (5) by a fictitious heat flux function $v(t)$. We will later present numerical experiments also for (18) when $B(x)$ is frozen in each time step, similar to [9] where the material parameters λ , c and ρ are frozen.

From (15) and the coercivity of σ_A we find that

$$\begin{aligned} \operatorname{Re}(A_\alpha \varphi, \varphi) &\leq -c_1 \|\varphi\|_{1,2}^2, \\ \operatorname{Re}(A_\alpha^* \varphi, \varphi) &\leq -c_1 \|\varphi\|_{1,2}^2. \end{aligned} \quad (19)$$

So A_α and A_α^* are densely defined, dissipative linear operators. By Proposition 1.1 we know that they are infinitesimal generators of \mathcal{C}^0 -semigroups $T_\alpha(t)$ and $T_\alpha^*(t)$. We note that by construction of $T_\alpha(t)$ the solution semigroup of the uncontrolled system is given by

$$T(t) = e^{\alpha t} T_\alpha(t) \quad (20)$$

which is generated by $A_T = A_\alpha + \alpha I$ on the domain of A_α . Analogously we see that

$$T^*(t) = e^{\alpha t} T_\alpha^*(t) \quad (21)$$

generated by $A_{T^*} = A_T^* = A_\alpha^* + \alpha I$. Furthermore from (19) we have

$$\|T(t)\| \leq e^{(\alpha - c_1)t} \text{ for } t \geq 0. \quad (22)$$

3.3 Approximation by Finite Dimensional Systems

Next we will treat the approximation of (16) by finite dimensional systems. A natural requirement for such approximations is

$$\forall \varphi \in H \exists \varphi^N \in H^N \text{ such that } \|\varphi - \varphi^N\| \leq \varepsilon(N) \text{ and } \varepsilon(N) \rightarrow 0 \text{ as } N \rightarrow \infty. \quad (\text{C1})$$

This is fulfilled by any Galerkin scheme based approximations, e.g. many finite element approximation schemes. In complete analogy to the procedure in (14) to (22) the restriction of σ_A to $H^N \times H^N$ leads to \mathcal{C}^0 -semigroups $T^N(t)$ and $T^N(t)^*$ generated by operators A_T^N and $A_{T^*}^N$ respectively. Let $P^N : L^2(\Omega) \rightarrow H^N$ be the canonical orthogonal projection onto H^N . We define the approximations B^N of B and Q^N of Q by

$$B^N = P^N B, \quad Q^N = P^N Q.$$

With these we define the approximating LQR-systems as

Minimize:

$$\mathcal{J}(x_0^N, u) := \int_0^\infty (x^N, Q^N x^N)_{H^N} + (u, Ru)_U dt, \quad (\mathcal{R}^N)$$

with respect to

$$\begin{aligned} M^N \dot{x}^N(t) &= A^N x^N(t) + B^N u(t), \text{ for } t > 0, \\ x^N(0) &= x_0^N \equiv P^N x_0 \end{aligned}$$

Note that in (\mathcal{R}^N) we already wrote the matrix representations of the finite dimensional operators in the fem-basis used for the spatial semi-discretization. This makes the mass matrix M^N appear on the left hand side of the state equation.

4 Theoretical Results

Before stating the main theoretical result we will first collect some approximation prerequisites we will need for the theorem. We call them **(BK1)** and **(BK2)** for they were already formulated in [1] (and called H1 and H2 there). The first and natural prerequisite is:

For each $x_0^N \in H^N$ there exists an admissible control $u^N \in L^2(0, \infty; U)$ for (\mathcal{R}^N) and any admissible control drives the state to 0 asymptotically. (BK1)

Additionally one needs the following properties of the finite dimensional approximations:

- (i) For all $\varphi \in H$ it holds $T^N(t)P^N\varphi \rightarrow T(t)\varphi$ uniformly on any bounded subinterval of $[0, \infty)$.
- (ii) For all $\phi \in H$ it holds $T^N(t)^*P^N\phi \rightarrow T(t)^*\phi$ uniformly on any bounded subinterval of $[0, \infty)$. (BK2)
- (iii) For all $v \in U$ it holds $B^N v \rightarrow Bv$ and for all $\varphi \in H$ it holds $B^{N*}\varphi \rightarrow B^*\varphi$.
- (iv) For all $\varphi \in H$ it holds $Q^N P^N \varphi \rightarrow Q\varphi$.

With these we can now formulate the main result.

Theorem 4.1 (Convergence of the finite dimensional approximations). *Let **(BK1)** and **(BK2)** hold. Moreover let $R > 0$, $Q \geq 0$ and $Q^N \geq 0$. Also let Π^N be the solutions of the AREs for the finite dimensional systems (\mathcal{R}^N) and let the minimal nonnegative self-adjoint solution Π of (\mathcal{R}) on H exist. Further let $S(t)$ and $S^N(t)$ be the operator semigroups generated by $A - BR^{-1}B^*\Pi$ on H and $A^N - B^N R^{-1} B^{N*} \Pi^N$ on H^N , respectively, with $\|S(t)\varphi\| \rightarrow 0$ as $t \rightarrow \infty$ for all $\varphi \in H$.*

If there exist positive constants M_1 , M_2 and ω independent of N and t , such that

$$\begin{aligned} \|S^N(t)\|_{H^N} &\leq M_1 e^{-\omega t}, \\ \|\Pi^N\|_{H^N} &\leq M_2, \end{aligned} \quad (23)$$

then

$$\begin{aligned} \Pi^N P^N \varphi &\rightarrow \Pi \varphi && \text{for all } \varphi \in H \\ S^N(t) P^N \varphi &\rightarrow S(t) \varphi && \text{for all } \varphi \in H \end{aligned} \quad (24)$$

converge uniformly in t on bounded subintervals of $[0, \infty)$ and it holds

$$\|S(t)\| \leq M_1 e^{-\omega t} \text{ for } t \geq 0. \quad (25)$$

Sketch of the Proof. This is basically [1, Theorem 2.2] which is formulated in terms of the sesquilinear forms and operator semigroups. In (14) to (22) we verified that the properties of the sesquilinear form and semigroups are preserved when migrating from distributed control (which Banks and Kunisch used) to boundary control. Therefore the proof boils down to that of [1, Theorem 2.2].

So we only have to verify the prerequisites (BK1), (BK2) and (23) here. Considering the fem basis representations (i.e. matrix representation) introduced in (\mathcal{R}^N) we find that (BK1) follows directly from well known results for finite dimensional regulator systems [14, 20]. The properties (iii) and (iv) of (BK2) are fulfilled by the Galerkin scheme underlying the finite element method used for the implementation. The first and second conditions follow from (20) and (21) together with

$$\begin{aligned} T_\alpha^N(t) P^N \varphi &\rightarrow T_\alpha(t) \varphi, \\ T_\alpha^N(t) P^{N*} \varphi &\rightarrow T_\alpha(t)^* \varphi, \end{aligned} \quad (26)$$

for all $\varphi \in H$ uniformly in t on any bounded subset of $[0, \infty)$. The later is basically an application of the Trotter-Kato Theorem. See [1, Lemma 3.2] and before for details. (23) is verified as in [1, Lemma 3.3]. \square

Theorem 4.1 gives the theoretical justification for the numerical method used for the linear problems described in this paper. It shows that the finite-dimensional closed-loop system obtained from optimizing the semi-discretized control problem indeed converges to the infinite-dimensional closed-loop system. Deriving a similar result for the nonlinear problems presented in Section 2.1 and also treated numerically in the following sections is an open problem.

5 Implementation details

We present different strategies of solving the control system here. We can divide them into two approaches. The first of which can be called the ODE approach, for it handles things just the way one would do in classical approaches concerning control systems governed by ordinary differential equations. The second one on the other hand closely follows the philosophy of finite element methods for parabolic partial differential equations and is therefore referred to as the PDE approach. Using the notation of semi-discretizations of partial differential equations one would call the ODE approach a vertical method of lines and the PDE approach a horizontal method of lines (Rothe method).

Both approaches need to solve an ARE to compute the control. This is done by the `LyaPack`¹ software package [18]. For further details on the theory of solving large sparse AREs and Lyapunov equations we refer the reader to [2, 3, 4, 13, 16, 17].

The basis of the finite dimensional approximations is given by the Galerkin scheme approximating the state space. This is achieved by a finite element semi-discretization of the spatial domain. We used the ALBERTA-1.2² [19] finite element library to do this. The macro triangulation that serves as the basis of the finite element approximation is shown in Figure 1. The curved surfaces at head and web of the profile are handled by a projection method, i.e., new boundary points are relocated to their appropriate position on a circular arc. The computational mesh is refined by a bisection refinement method.

We start both approaches with a short uncontrolled forward calculation. During this calculation the profile is cooled down from constant 1000°C until the maximal temperature reaches approximately 990°C to have a more realistic temperature distribution at the control startup. This calculation is done with boundary conditions set up to model cooling in surrounding air of 20°C. See [6, Section 4] for information on the chosen heat transfer coefficients.

Finishing the *pre*-calculation we end up with an initial set of system matrices A^N , B^N , C^N and M^N . These are then used to compute the feedback matrix K with the `LyaPack` software using a MATLAB `mexfunction` implemented for this purpose.

In the ODE approach the matrix K is used to establish the closed loop system

$$\begin{aligned} M^N \dot{x}(t) &= -(A^N + B^N K^T)x(t), \\ x(0) &= x_0. \end{aligned} \tag{27}$$

The solution of the closed loop system can then be calculated by a standard ODE solver like `ode23` of MATLAB.

The PDE approach uses K to set up the boundary conditions. Doing this we have the full space adaption capabilities of ALBERTA at hand to refine or coarsen the mesh as needed. On the other hand we have to pay for this freedom by frequent recalculations of K if the mesh and with it the system matrices M^N , A^N and B^N have changed. At the moment we solve this problem by calculating certain control parameters (i.e. the temperature of the cooling fluid or the intensity parameters for the cooling nozzles depending on the boundary conditions used) and freezing them for a number of timesteps preset by the user.

Numerical calculations with updates after 2, 5 and 10 timesteps show that parameters tend to become *the same* after 10-20 seconds in model time, even if we use an implicit time integration scheme with probably *large* timesteps. Thus all update strategies lead to the same asymptotic behavior. See Figure 2 for a plot of the control parameters (temperatures of the cooling fluid) over time. The term *the same* is to be understood as “equal regarding model accuracy”, for

¹available at <http://www.tu-chemnitz.de/sfb393/lyapack>

²available at <http://www.alberta-fem.de>.

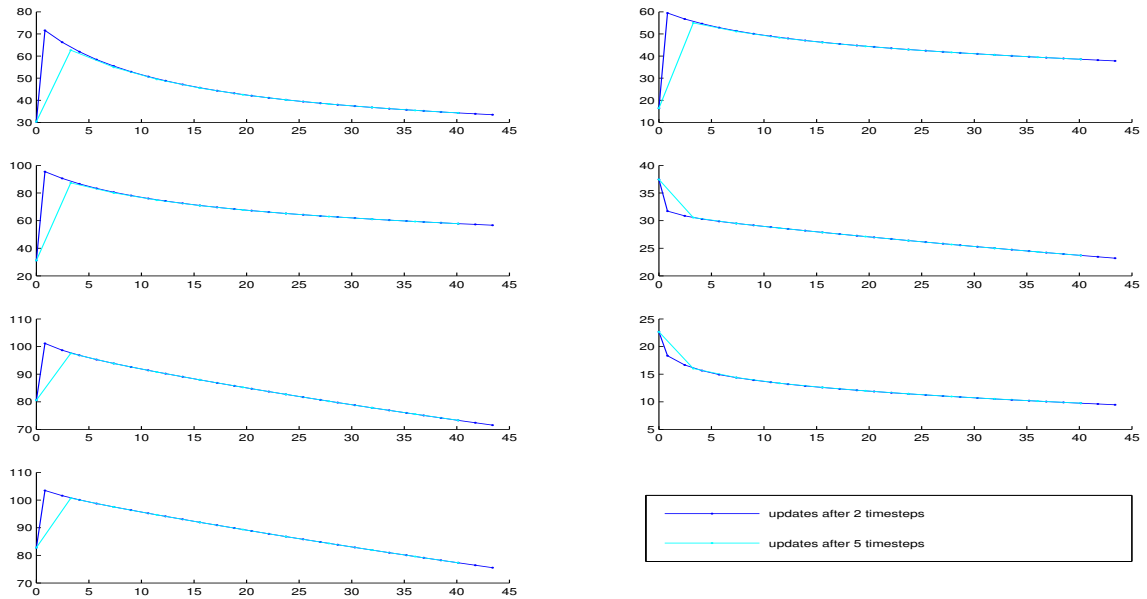


Figure 2: Temperatures of the cooling fluid (i.e. control parameters) plotted over time for different update frequencies

temperature differences in the size of deci- or even centi-°C for the cooling fluid should be referred to as equal concerning technical application of the computed controls.

Even using the spraying intensities as controls which leads to a bilinear control system with state dependent input matrix $B(x)$, can be computed by this method leading to promising results. To do this we linearize the system by choosing $B := B(x(t_n))$ on the time interval $\tau_n := [t_n, t_{n+1}]$. Interpreting this method in terms of instantaneous control or model predictive control is future work and will be presented elsewhere.

6 Numerical results

We will now present selected numerical results. In order to not go beyond the scope of this paper we can not present all the tests we have made. Some results for computations with differing cost functionals can be found in [5]. There the cost functional is changed by means of the output matrix C .

In Figure 3 the initial condition and the mesh for our computations are shown. This is the state after the preliminary forward calculation discussed in Section 5. We chose a different color-bar here because the color-bar used for the other figures is much too bright for the initial condition and one would not be able to see anything otherwise. On the other hand the color-bar used for the initial condition has non monotonic brightness characteristics, which makes it unusable for

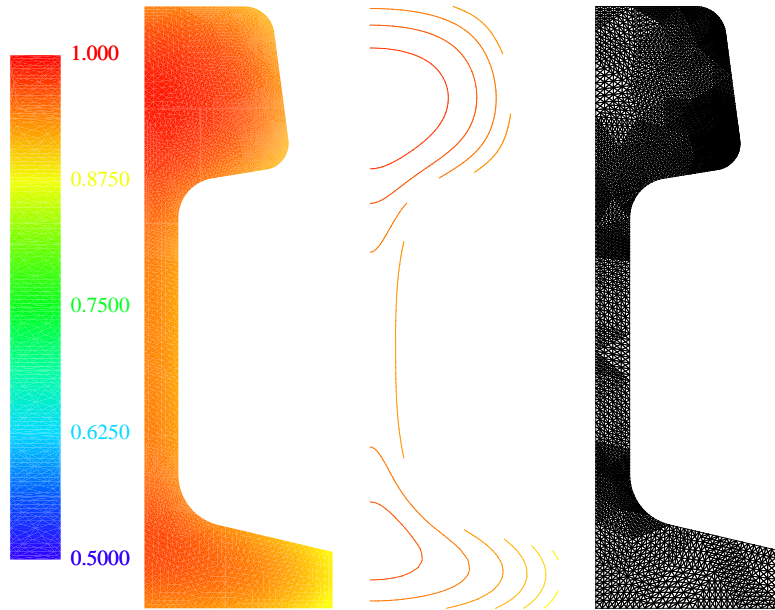


Figure 3: initial condition and computational mesh of the numerical tests

black and white printouts. Note that the color-bar used in Figures 4–5 uses white and yellow for the hottest state and red to black for the lower temperatures. So red areas are the *cold* ones here. The printed mesh is held constant for the computations done here. The mesh is derived from that of Figure 1 by 2 global refinements using a bisection refinement method (See [19, Section 1.1] for details on this method.) resulting in 5177 grid nodes. This corresponds to 5177 degrees of freedom since we used linear polynomial elements.

In Figure 4 the results for calculations with different levels of nonlinearity in the model and control system are shown³. The term *nonlinear boundary condition* refers to boundary condition (5) with κ_k as the control, which is nonlinear in the sense that it leads to the bilinear control system. In the figure one should primarily look at the results till $t = 30$ seconds. The results for $t = 40$ seconds show temperatures much lower than 700°C and are therefore already exceeding model limitations. So the plots for $t = 40$ seconds should be seen as qualitative images of the real behavior rather than quantitatively correct. See Figure 5 for comparison with an uncontrolled reference run of the linearized model. That run continues the preliminary run for an additional 45 seconds of model time.

Note that in contrast to Figure 2 in Figures 3–5 the data (temperature and time) is rescaled as described in Section 2.5. Computations for the linear boundary conditions (control via temperature of the cooling fluid) have been done with C according to (7), $R = 0.1I$ and $\hat{Q} = 7.5 \cdot 10^{-4}I$. The computations for the nonlinear boundary condition use the same C , but $R = 10^{-3}I$ and $\hat{Q} = 10^{-4}I$. We do not give any computation times here, because we

³Animations of the cooling process can be found at <http://www.tu-chemnitz.de/mathematik/industrietechnik/projekte/lqrpde.e.php>

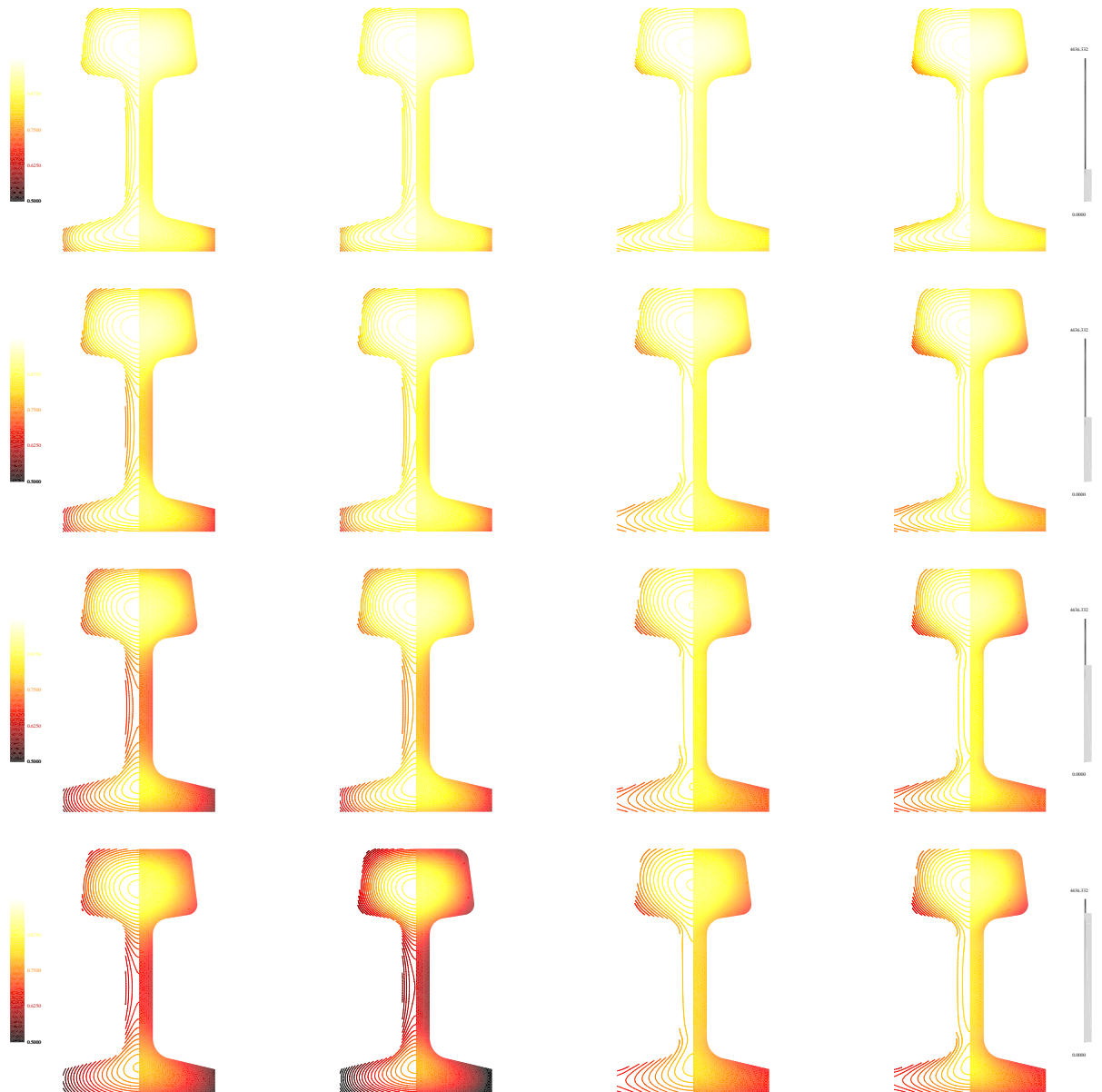


Figure 4: Temperature distributions on cross-sections of the profile. Left to right: linear equation with linear boundary conditions, nonlinear equation with linear boundary conditions, linear equation with nonlinear boundary conditions and nonlinear equation with nonlinear boundary conditions. Top to bottom: snapshots after 10, 20, 30 and 40 seconds.

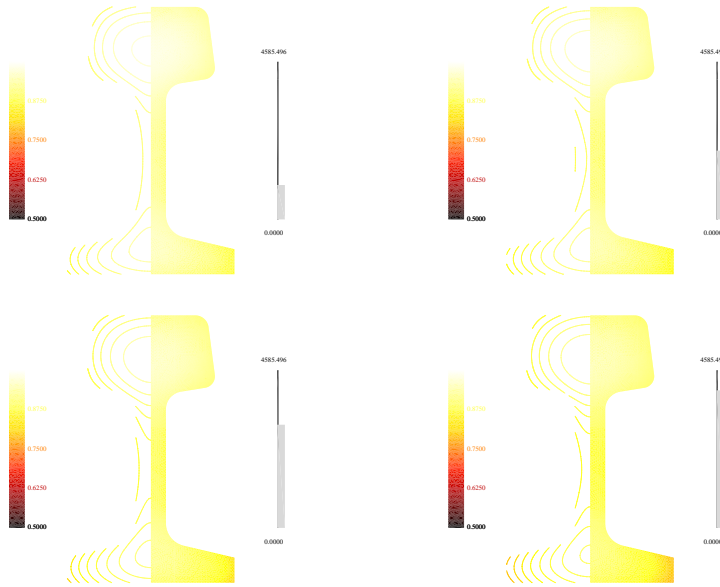


Figure 5: uncontrolled reference run modeling cooling in air of 21°C for the linearized model

do not have a standalone implementation yet. The mex interface and conversion of sparse matrix formats between ALBERTA- and MATLAB-formats produce noticeable overhead and a standalone C version which directly uses the linear system solvers included in ALBERTA should perform much better than having MATLAB as additional overhead.

The obtained data can be interpreted as follows. Obviously, differences arise merely from going from linear to nonlinear boundary conditions rather than using nonlinear model equations. It appears as if with the linear boundary conditions, heat is taken out of the profile faster than to be realistic. Generally our results qualitatively compare well to those of [9, 21, 11]. Quantitative statements are difficult because of the different initial conditions used. At least we observe the same cooling rates in our approach, i.e., we achieve temperature reductions very similar to those in the above publications in comparable times. This demonstrates that an LQR-based control design is competitive to other control strategies suggested for this application.

7 Conclusions

We have presented theoretically efficient optimal control methods for the approximation of infinite-dimensional LQR problems. Some of the simulation results still require theoretical backing. The adequate results and the expansion of the numerical approaches to the 3-dimensional case, as well as an optimized implementation to obtain competitive calculation times are the topic of current research. The chosen application demonstrates that the LQR approach works well for the steel cooling process and is competitive to other control strategies based on optimization techniques. The presented strategy should work even better for appli-

cations like air-conditioning, stabilization of Euler-Bernoulli beams or alike, where nonlinear effects are less important. This will also be investigated further in future work. In general, the framework of addressing optimal control problems for parabolic problems by an LQR approach based on an efficient implementation of the corresponding computational tools, can be applied to a wide variety of control problems for linear evolution problems.

References

- [1] H. T. BANKS AND K. KUNISCH, *The linear regulator problem for parabolic systems*, SIAM J. Cont. Optim., 22 (1984), pp. 684–698. 7, 11, 12
- [2] P. BENNER, *Efficient algorithms for large-scale quadratic matrix equations*, Proc. Appl. Math. Mech., 1 (2002), pp. 492–495. 13
- [3] ———, *Solving large-scale control problems*, IEEE Control Systems Magazine, 14 (2004), pp. 44–59. 13
- [4] P. BENNER, J.-R. LI, AND T. PENZL, *Numerical solution of large Lyapunov equations, Riccati equations, and linear-quadratic optimal control problems*. Unpublished manuscript, December 1999. 1, 13
- [5] P. BENNER AND J. SAAK, *Efficient numerical solution of the LQR-problem for the heat equation*, Proc. Appl. Math. Mech., (2004). 6, 14
- [6] M. BÖHM, M. WOLFF, E. BÄNSCH, AND D. DAVIS, *Modellierung der Abkühlung von Stahlbrammen, Berichte aus der Technomathematik, Bericht 00-07*. <http://www.math.uni-bremen.de/zetem/reports/reports-psgz/report0007.ps.gz>, 2000. 13
- [7] K.-J. ENGEL AND R. NAGEL, *One-parameter semigroups for linear evolution equations.*, vol. 194 of Graduate Texts in Mathematics, Springer-Verlag, Berlin, 2000. 2
- [8] K. EPPLER AND F. TRÖLTZSCH, *Discrete and continuous optimal control strategies in the selective cooling of steel profiles*, Z. Angew. Math. Mech., 81 (2001), pp. 247–248. 1, 3
- [9] ———, *Discrete and continuous optimal control strategies in the selective cooling of steel profiles*, Preprint 01-3, DFG Schwerpunktprogramm *Echtzeit-Optimierung großer Systeme*, 2001. Available from <http://www.zib.de/dfg-echtzeit/Publikationen/Preprints/Preprint-01-3.html>. 1, 3, 10, 17
- [10] J. GIBSON, *The Riccati integral equation for optimal control problems on Hilbert spaces*, SIAM J. Cont. Optim., 17 (1979), pp. 537–565. 7, 8
- [11] R. KRENGEL, R. STANDKE, F. TRÖLTZSCH, AND H. WEHAGE, *Mathematisches Modell einer optimal gesteuerten Abkühlung von Profilstählen in Kühlstrecken*, Preprint 98-6, Fakultät für Mathematik TU Chemnitz, November 1997. 1, 3, 17

- [12] I. LASIECKA AND R. TRIGGIANI, *Control Theory for Partial Differential Equations: Continuous and Approximation Theories I. Abstract Parabolic Systems*, Cambridge University Press, Cambridge, UK, 2000. 7
- [13] J.-R. LI AND J. WHITE, *Low rank solution of Lyapunov equations*, SIAM J. Matrix Anal. Appl., 24 (2002), pp. 260–280. 13
- [14] A. LOCATELLI, *Optimal Control: an Introduction*, Birkhäuser, Basel, Boston, Berlin, 2001. 12
- [15] A. PAZY, *Semigroups of linear operators and applications to partial differential equations.*, Applied Mathematical Sciences, 44. New York etc.: Springer-Verlag. VIII, 1983. 2
- [16] T. PENZL, *A cyclic low rank Smith method for large, sparse Lyapunov equations with applications in model reduction and optimal control*, Tech. Rep. SFB393/98-6, Sonderforschungsbereich 393 *Numerische Simulation auf massiv parallelen Rechnern*, TU Chemnitz, 09107 Chemnitz, FRG, 1998. Available from <http://www.tu-chemnitz.de/sfb393/sfb98pr.html>. 13
- [17] ———, *A cyclic low rank Smith method for large sparse Lyapunov equations*, SIAM J. Sci. Comput., 21 (2000), pp. 1401–1418. 13
- [18] ———, *LYAPACK Users Guide*, Tech. Rep. SFB393/00-33, Sonderforschungsbereich 393 *Numerische Simulation auf massiv parallelen Rechnern*, TU Chemnitz, 09107 Chemnitz, FRG, 2000. Available from <http://www.tu-chemnitz.de/sfb393/sfb00pr.html>. 13
- [19] A. SCHMIDT AND K. SIEBERT, *Design of Adaptive Finite Element Software. The Finite Element Toolbox ALBERTA*, vol. 42 of Lecture Notes in Computational Science and Engineering, Springer-Verlag, Berlin-Heidelberg, 2005. 13, 15
- [20] E. SONTAG, *Mathematical Control Theory*, Springer-Verlag, New York, NY, 2nd ed., 1998. 12
- [21] F. TRÖLTZSCH AND A. UNGER, *Fast solution of optimal control problems in the selective cooling of steel*, Z. Angew. Math. Mech., 81 (2001), pp. 447–456. 1, 3, 17
- [22] J. WLOKA, *Partial differential equations.*, Cambridge University Press. XI, 1987. Transl. from the German by C. B. and M. J. Thomas. 2, 9

Other titles in the SFB393 series:

- 03-01 E. Creusé, G. Kunert, S. Nicaise. A posteriori error estimation for the Stokes problem: Anisotropic and isotropic discretizations. January 2003.
- 03-02 S. I. Solov'ëv. Existence of the guided modes of an optical fiber. January 2003.
- 03-03 S. Beuchler. Wavelet preconditioners for the p-version of the FEM. February 2003.
- 03-04 S. Beuchler. Fast solvers for degenerated problems. February 2003.
- 03-05 A. Meyer. Stable calculation of the Jacobians for curved triangles. February 2003.
- 03-06 S. I. Solov'ëv. Eigenvibrations of a plate with elastically attached load. February 2003.
- 03-07 H. Harbrecht, R. Schneider. Wavelet based fast solution of boundary integral equations. February 2003.
- 03-08 S. I. Solov'ëv. Preconditioned iterative methods for monotone nonlinear eigenvalue problems. March 2003.
- 03-09 Th. Apel, N. Düvelmeyer. Transformation of hexahedral finite element meshes into tetrahedral meshes according to quality criteria. May 2003.
- 03-10 H. Harbrecht, R. Schneider. Biorthogonal wavelet bases for the boundary element method. April 2003.
- 03-11 T. Zhanlav. Some choices of moments of refinable function and applications. June 2003.
- 03-12 S. Beuchler. A Dirichlet-Dirichlet DD-pre-conditioner for p-FEM. June 2003.
- 03-13 Th. Apel, C. Pester. Clément-type interpolation on spherical domains - interpolation error estimates and application to a posteriori error estimation. July 2003.
- 03-14 S. Beuchler. Multi-level solver for degenerated problems with applications to p-version of the fem. (*Dissertation*) July 2003.
- 03-15 Th. Apel, S. Nicaise. The inf-sup condition for the Bernardi-Fortin-Raugel element on anisotropic meshes. September 2003.
- 03-16 G. Kunert, Z. Mghazli, S. Nicaise. A posteriori error estimation for a finite volume discretization on anisotropic meshes. September 2003.
- 03-17 B. Heinrich, K. Pönitz. Nitsche type mortaring for singularly perturbed reaction-diffusion problems. October 2003.
- 03-18 S. I. Solov'ëv. Vibrations of plates with masses. November 2003.
- 03-19 S. I. Solov'ëv. Preconditioned iterative methods for a class of nonlinear eigenvalue problems. November 2003.
- 03-20 M. Randrianarivony, G. Brunnett, R. Schneider. Tessellation and parametrization of trimmed surfaces. December 2003.
- 04-01 A. Meyer, F. Rabold, M. Scherzer. Efficient Finite Element Simulation of Crack Propagation. February 2004.
- 04-02 S. Grosman. The robustness of the hierarchical a posteriori error estimator for reaction-diffusion equation on anisotropic meshes. March 2004.

- 04-03 A. Bucher, A. Meyer, U.-J. Görke, R. Kreißig. Entwicklung von adaptiven Algorithmen für nichtlineare FEM. April 2004.
- 04-04 A. Meyer, R. Unger. Projection methods for contact problems in elasticity. April 2004.
- 04-05 T. Eibner, J. M. Melenk. A local error analysis of the boundary concentrated FEM. May 2004.
- 04-06 H. Harbrecht, U. Kähler, R. Schneider. Wavelet Galerkin BEM on unstructured meshes. May 2004.
- 04-07 M. Randrianarivony, G. Brunnett. Necessary and sufficient conditions for the regularity of a planar Coons map. May 2004.
- 04-08 P. Benner, E. S. Quintana-Ortí, G. Quintana-Ortí. Solving Linear Matrix Equations via Rational Iterative Schemes. October 2004.
- 04-09 C. Pester. Hamiltonian eigenvalue symmetry for quadratic operator eigenvalue problems. October 2004.
- 04-10 T. Eibner, J. M. Melenk. An adaptive strategy for hp-FEM based on testing for analyticity. November 2004.
- 04-11 B. Heinrich, B. Jung. The Fourier-finite-element method with Nitsche-mortaring. November 2004.
- 04-12 A. Meyer, C. Pester. The Laplace and the linear elasticity problems near polyhedral corners and associated eigenvalue problems. December 2004.
- 04-13 M. Jung, T. D. Todorov. On the Convergence Factor in Multilevel Methods for Solving 3D Elasticity Problems. December 2004.
- 05-01 C. Pester. A residual a posteriori error estimator for the eigenvalue problem for the Laplace-Beltrami operator. January 2005.
- 05-02 J. Badía, P. Benner, R. Mayo, E. Quintana-Ortí, G. Quintana-Ortí, J. Saak. Parallel Order Reduction via Balanced Truncation for Optimal Cooling of Steel Profiles. February 2005.
- 05-03 C. Pester. CoCoS – Computation of Corner Singularities. April 2005.
- 05-04 A. Meyer, P. Nestler. Mindlin-Reissner-Platte: Einige Elemente, Fehlerschätzer und Ergebnisse. April 2005.
- 05-05 P. Benner, J. Saak. Linear-Quadratic Regulator Design for Optimal Cooling of Steel Profiles. April 2005.

The complete list of current and former preprints is available via
<http://www.tu-chemnitz.de/sfb393/preprints.html>.